14

Power Electronics Application for More Electric Aircraft

Mohamad Hussien Taha
Hariri Canadian University
Lebanon

1. Introduction

In the competitive world of airline economics, where low cost carriers are driving dawn profit margins on airline seat miles, techniques for reducing the direct operating costs of aircraft are in great demand. In effort to meet this demand, the aircraft manufacturing industry is placing greater emphasis on the use of technology, which can influence maintenance costs and fuel usage. (Faleiro, 2005)

There is a general move in the aerospace industry to increase the amount of electrically powered equipments on future aircraft. This trend is referred to as the "More Electric Aircraft". It assumes using electrical energy instead of hydraulic, pneumatic and mechanical means to power virtually all aircraft subsystem including flight control actuation, environmental control system and utility function. The concept offers advantages of reduced overall aircraft weight, reduced need for ground support equipment and maintenance and increased reliability (Taha,2007,Wiemer,1999).

Many aircraft power systems are now operating with a variable frequency over a typical range of 360 Hz to 800 Hz.

Distribution voltages for an aircraft system can be classified as:

a. Nominal 115/200 V rms and 230/400 V rms ac, both one phase and three phase, over variable frequency range.
b. Nominal 14, 28 and 42 V DC.
c. High DC voltage which could be suitable for use with an electric actuator (or other) aircraft loads.

This chapter presents studies, analysis and simulation results for a boost and buck converters at variable input frequency using vector control scheme. The design poses significant challenges due to the supply frequency variation and requires many features such as:

1. The supply current to the converter must have a low harmonic contents to minimize its impact on the aircraft variable frequency electrical system.
2. A high input power factor must be achieved to minimize reactive power requirements.
3. Power density must be maximized for minimum size and weight.

2. Boost converter for aircraft application

A three phase boost converter which is shown in fig. 1 with six steps PWM provide DC output and sinusoidal input current with no low frequency harmonic. However the switching frequency harmonics contained in the input currents must be suppressed by the input filter. Referring to fig.1 after the output capacitor has charged up via the diodes to a voltage equals to $1.73V_{pk}$, the diodes are all reverse biased. Turning one of the MOSFETs in each of the three phases will cause the inductor current to increase. Assume the input voltage V_a is positive, if S_2 is turned on, the inductor current increases through the diode D_4 or D_6 and the magnetic energy is stored in the inductor. Since the diodes D_1, D_3 and D_5 are reverse biased, the output capacitor C_{dc} provides the power to the load. When S_2 is turned off, the stored energy in the inductor and the AC source are transferred to C_{dc} and the load via the diodes. When the AC voltage is negative, S_1 is turned on and the inductor current increases through the diode D_3 or D_5. The same operation modes are involved for phase B and phase C (Taha., 2008; Habetler.,1993). Fig.2 and fig. 3 show different operating modes.

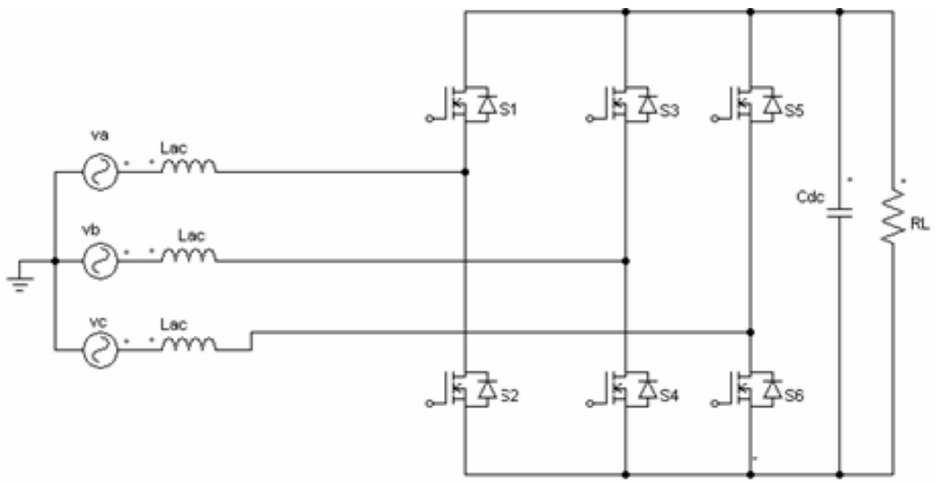

Fig. 1. Boost converter.

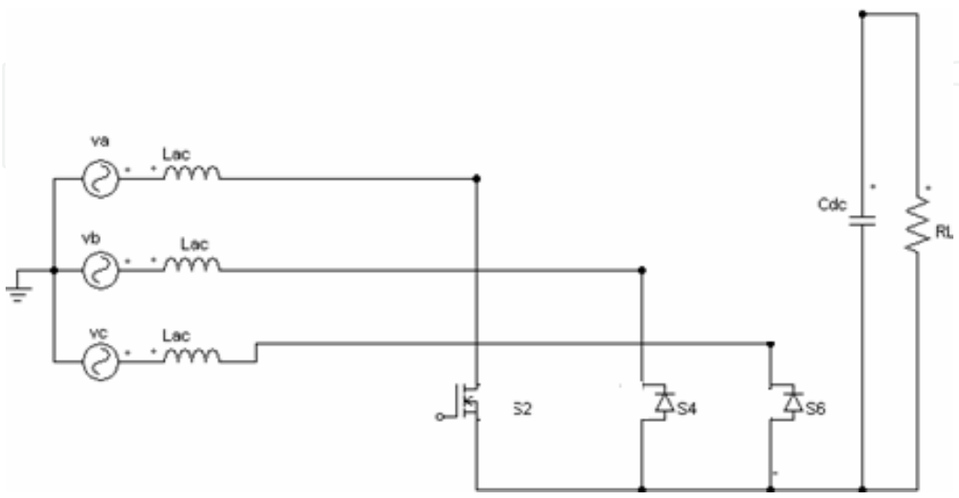

Fig. 2. Boost converter when V_a is positive.

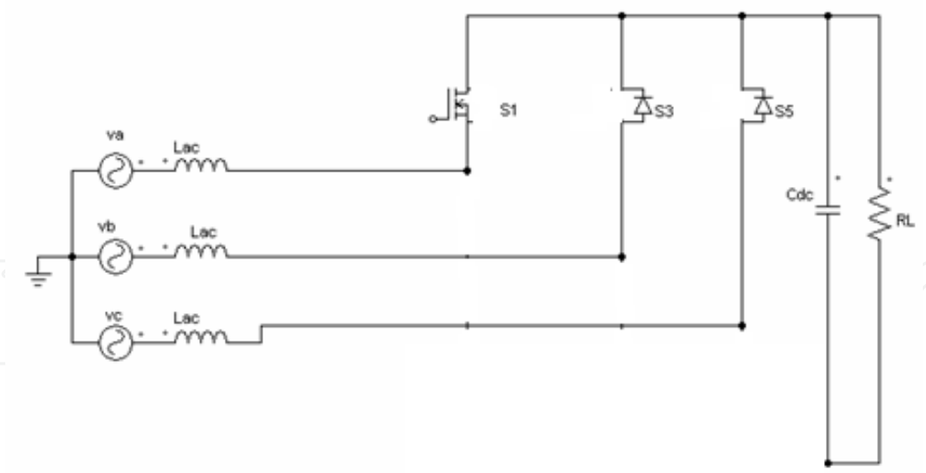

Fig. 3. Boost converter when V_a is negative.

3. Buck converter for aircraft application

The buck 3-phase/dc converter is a controlled current circuit which relies on pulse width modulation of a constant current to achieve low distortion. As shown in fig. 4. The circuit consists of 3 power MOSFETs and 12 diodes, an AC side filter and DC side filter.

The AC side input and DC side output filters are standard second order low pass L-C filters. For the input filter, the carrier frequency has to be considerably higher than the filter resonance frequency in order to avoid resonance effects and ensure carrier attenuation. The Ac side filter is arranged to bypass the commutating energy when the MOSFETs are turning off and to absorb the harmonic for the high frequency switching. At the DC side, the inductor is used to maintain a constant current, this inductor can be relatively small since the ripple frequency will be related to the switching frequency. The magnitude and the phase of the input current can be controlled and hence the power transfer that occurs between the AC and DC sides can also be controlled. (Green et al., 1997).

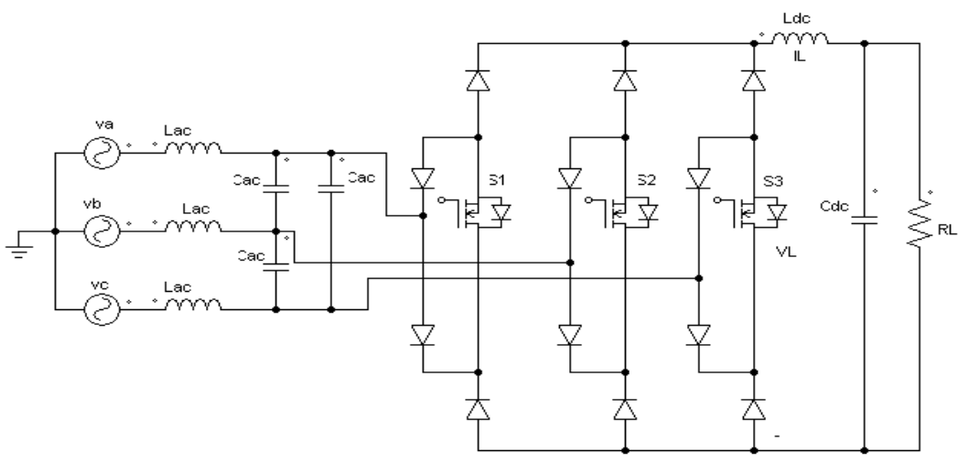

Fig. 4. Buck converter.

The input phase voltages V_a, V_b, V_c and the input currents I_a, I_b, I_c are assumed to be sinusoidal of equal magnitude and symmetrical

$$V_a = V_{pk} \sin(\omega t) \quad I_a = I_{pk} \sin(\omega t + \varphi) \tag{1}$$

$$V_b = V_{pk} \sin(\omega t - 2\pi/3) \quad I_b = I_{pk} \sin(\omega t - 2\pi/3 + \varphi) \tag{2}$$

$$V_c = V_{pk} \sin(\omega t + 2\pi/3) \quad I_c = I_{pk} \sin(\omega t + 2\pi/3 + \varphi) \tag{3}$$

Figure (5) shows 60 degrees of two sine waveforms.

$$T_a = TM \sin(\omega t + \varphi) \tag{4}$$

$$T_b = TM \sin(\omega t + 2\pi/3 + \varphi) \tag{5}$$

The freewheeling time T_f is equal to:

$$T_f = T - T_a - T_b \tag{6}$$

Where: φ is the displacement angle,
Vpk is the peak phase voltage,.
M modulation index.
T is the PWM switching period.

The general operation of the system is as follows: The switching of the devices is divided into six equal intervals of the 360 degrees main cycle. The waveforms repeat a similar pattern at each interval. At any time during the switching interval, only two converter legs are modulated independently and the third leg is always on. There are some time intervals that only one device is only on, thus providing a freewheeling for the DC current since at this time the energy stored on the DC inductor feeds the load.

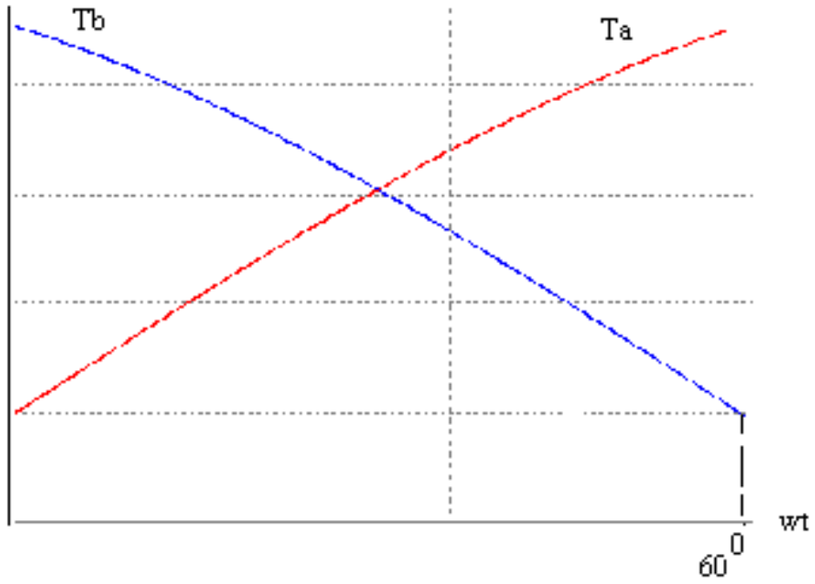

Fig. 5. Two 60° sine waves.

Mode 1

With S_2 on and S_1 is modulated by reference T_a, current flows in phase (a) and phase (b). $I_a>0$ and $I_b<0$, The bridge output voltage V_L is connected to main line supply V_{ab} which opposed by V_{DC} is applied across the inductor. Current I_L increases in the inductor.

$$I_L = I_a = -I_b \tag{7}$$

$$V_L = V_{ab} \tag{8}$$

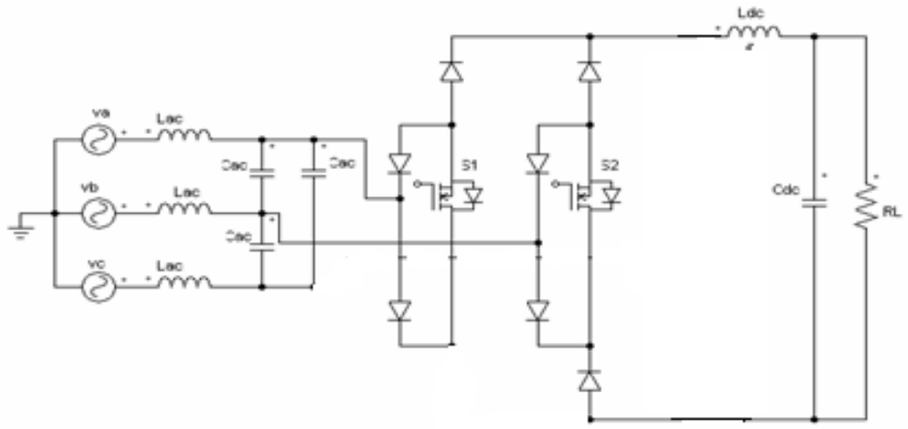

Fig. 6. Mode 1 equivalent circuit.

Mode 2

With S_2 on and S_3 is modulated by T_b, current flows in phase (c) and phase (b). $I_c>0$ and $I_b<0$. Line voltage V_{cb} opposed by V_{DC} is applied across the inductor. Again the inductor current increases.

$$I_L = I_c = -I_b \tag{9}$$

$$V_L = V_{cb} \tag{10}$$

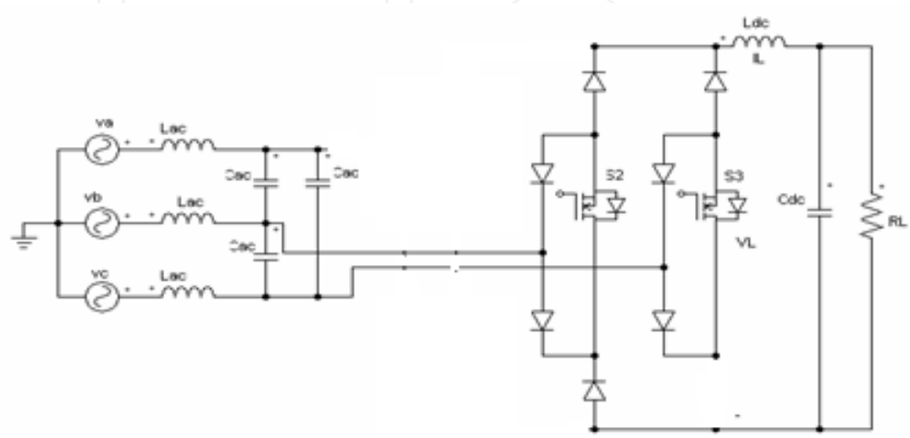

Fig. 7. Mode 2 equivalent circuit.

Mode 3

In this mode, only one MOSFET is on (S_2), the inductor current freewheels and the converter is disconnected from the mains and the DC voltage is zero.

$$V_L = 0 \tag{11}$$

Therefore the average voltage V_L over one switching period T is:

$$V_L = [(V_{ab} \times T_a) + (V_{cb} \times T_b)] / T \tag{12}$$

Where:

$$V_{ab} = V_a - V_b = 1.5V_{pk} \sin(\omega t) + 0.866\, V_{pk} \cos(\omega t) \tag{13}$$

$$V_{cb} = V_c - V_b = 1.73\, V_{pk} \cos(\omega t) \tag{14}$$

By substituting equations 8, 10, 12 and 13 into equation 12 yeilds:

$$V_L = V_{DC} = [(V_{ab} \times T_a) + (V_{cb} \times T_b)] / T = 1.5\, M\, V_{pk} \cos\varphi \tag{15}$$

By assuming an ideal power converter in which the power losses are negligible, the power nput is then equal to power output, and by assuming $\cos\varphi = 1$, The DC output voltage can be defined as :

$$V_{DC} = 1.5\, M\, V_{pk} \tag{16}$$

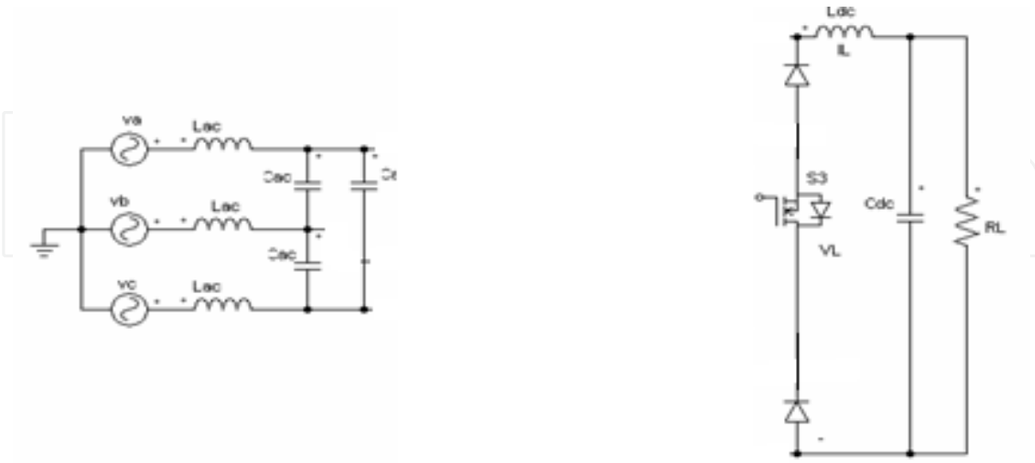

Fig. 8. Mode 3 equivalent circuit.

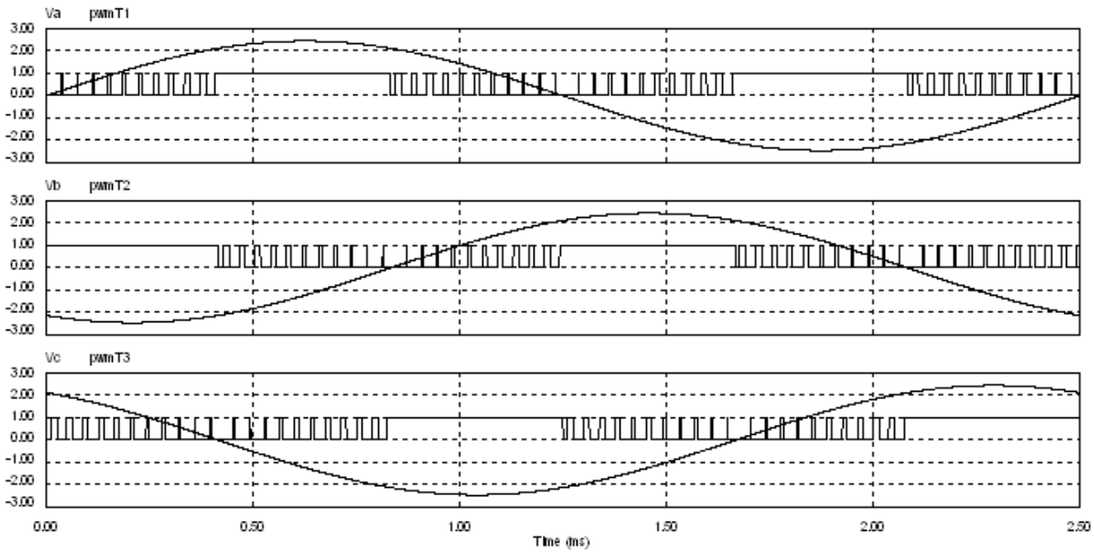

Fig. 9. PWM for the buck converter.

4. Adaptive reactive power control using boost converter

In comparison to the operating frequencies of land based power systems, which is normally 50-60 Hz, the operation of aircraft power systems at these relatively high frequencies can present some technical difficulties. One area of importance is associated with the impedance of the potentially long cables (which may run along part of the wing and a large proportion of the fuselage). These cables connect electrical loads, such as electric actuators for aircraft flight surfaces, to the AC supply, or "point of regulation" (POR). In large modern aircraft, the cables can be in excess of 200 ft and contribute impedance which is dependent on the cable's inductance and resistance. The inductive reactance, X_L, is proportional to the operating frequency of the power system and is given by $X_L = 2\pi fL$, where f is the operating frequency and L is the inductance of the cable and therefore the reactance changes with operating frequency. (Taha M, Trainer R D 2004). As the connected load draws a current, the cable develops a voltage drop due to its impedance which is out of phase with respect to the voltage at the POR and has two detrimental effects:

The voltage at the load is reduced below the regulated voltage at the point of regulation which is usually at the generator output.

The power factor of the load seen at the point of regulation reduces (even for a purely resistive load).

The voltage drop across the cable is clearly disadvantageous. The voltage drop may be tolerated and the connected loads have to be correspondingly down rated for the lower received voltage. Alternatively the voltage drop across the length of the cable is not allowed to exceed a threshold (typically 4 V) and it is necessary to provide cables that are both large and heavy such that their resistance remains low. Clearly space and weight are at a premium in aerospace applications. There can be significant weight saving if smaller, high resistance cables are used, particularly where low duty cycle, pulsed loads like electric

actuators are supplied. The detrimental effects of such cables may be offset if the system designer uses the high inductive reactance present at the higher operating frequencies to affect voltage boost and power factor correction.

The simplest type of compensation for this type of problem is to connect a set of 3-phase capacitors (star or delta) at the point of connection of the load, in a similar way to ac motor-start capacitors. The capacitors can be used as a generator of reactive power but the beneficial effects are limited since the capacitive compensation is mainly controlled by the voltage magnitude and system frequency rather than the requirements of the load. Having noted the limitations of connecting shunt capacitors, there may be some applications where this type of compensation is applicable.

There is growing interest in the use of advanced power electronic circuits for aerospace loads, particularly in the motor-drives associated with electric actuators. The main two classes of converters currently being considered are active rectifiers and direct ac-ac frequency changer circuits (e.g. Matrix converters). Both types of converter can be made to operate with leading, lagging or unity power factor by suitable control of the semi-conductor switching elements.

The current view in the aerospace industry appears to be that the operation of these converters should be limited to unity power factor and little (or no) work has been carried out to explore the true system level benefits of variable power factor operation.

Fig.10 shows a basic circuit diagram for an electric actuator load incorporating an advanced power electronic converter with power factor control. It is clear that by controlling the power factor of the converter (shown leading), the effects of cable inductance can be eliminated so that the load as seen from the POR becomes unity power factor. Other operating power factors may be desirable in order to optimize the operation of the overall power system, including the generator loading.

Because the effects are proportional to the load current flowing through the cable and the system frequency, the reactive power compensation provided by the converter also needs to be variable.

The voltage magnitude at the load can be made the same as that at the POR. It could be beneficial in some applications to boost the input voltage by increasing the capacitive compensation provided by the power electronic converter.

The main benefit of using the advanced power electronic converter as a source of reactive power is to reduce (or eliminate) the voltage drop down the connecting cable. This gives us the possibility to use high impedance cables with benefits of reduced conductor diameter and significantly lower weight.

In order to understand the benefits of reactive power control, it is convenient to consider the flow of real and reactive current separately as shown in figure 10. Superposition can then be used to assess the net effect of both forms of current flow.

Therefore:

$$i = i_p + ji_q = I\,(\cos\theta_1 + j\sin\theta_1) \tag{17}$$

Where

$$\theta_1 = \tan^{-1}(i_q / i_p) \tag{18}$$

$$E = V + (i_p + ji_q)R + (i_p + ji_q)jX_L \tag{19}$$

$$E = V + i_p R - i_q X_L + j(i_q R + i_p X_L) \tag{20}$$

$$E = E((\cos\theta_2 + j\sin\theta_2) \tag{21}$$

Where

$$\theta_2 = \tan^{-1}((i_q R + i_p X_L)/ (V + i_p R - i_q X_L)) \tag{22}$$

For unity power factor θ_1 should equals θ_2.
Therefore:

$$(i_q / i_p) = (i_q R + i_p X_L)/ (V + i_p R - i_q X_L) \tag{23}$$

$$i_q = ((V/ X_L) \pm ((V/ X_L)^2 - 4\, i_p^2)^{1/2})/2 \tag{24}$$

In a practical system, ip could take the form of a current demand and iq would be a separate reactive current demand that is made to vary as a function of ip and X_L (frequency dependant). R and X_L are cable dependant parameters.

Referring to Fig. 10, the inputs here are system frequency and load current, the output is Q demand, which is an input to the power electronic converter. The parameters of the cable are stored and used within the electronic circuitry to calculate the required compensation for the system under consideration.

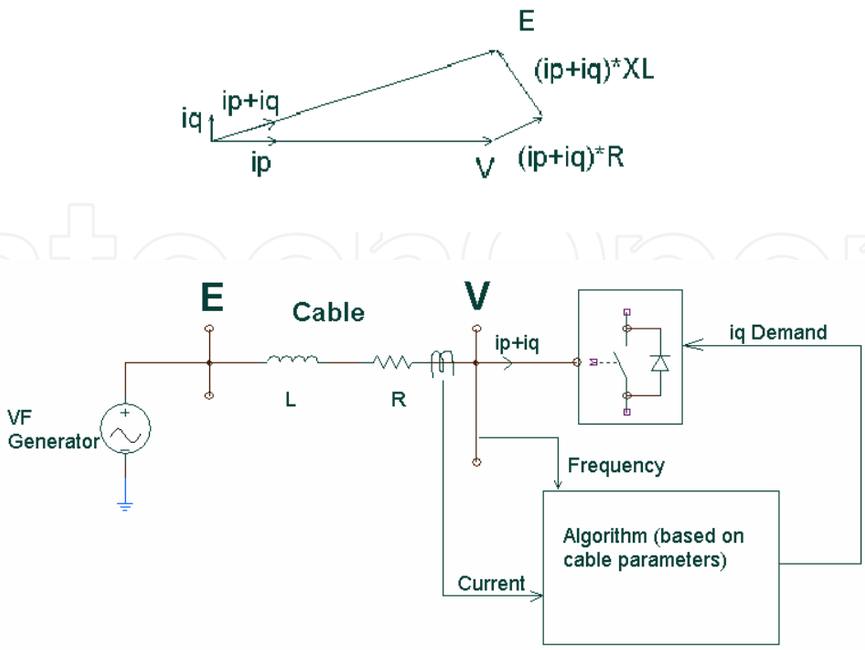

Fig. 10. System performance for reactive power compensation.

5. DQ vector control for the converters

In the DQ vector control strategy the instantaneous 3 phase voltages and currents are transferred to a 2-axis reference frame system which rotates at the angular frequency of the supply. This has the effect of transforming the three phase AC quantities (representing rotating volt and current phasors in the stationary co-ordinate frame) into DC quantities in the synchronously rotating frame (Taha et al.,2002, Taha,. 2008). If the D axis is chosen to be aligned with the voltage phasor, the D and Q axis current components represent the active and reactive components respectively. Fig. 11 shows the schematic of the DQ control scheme implemented in the input converter.

The proposed control scheme consists of two parts:

1. An outer voltage controller.
2. An inner current controller.

The outer voltage controller regulates the DC link voltage. The error signal is used as input for the PI voltage controller this provides a reference to the D current of the inner current controller. The Q current reference is set to zero to give unity power factor. A PI inner current control is used to determine the demand of the stationary DQ voltage values (Taha M & Trainer R D 2004; Kazmierkoski et al., 1991).

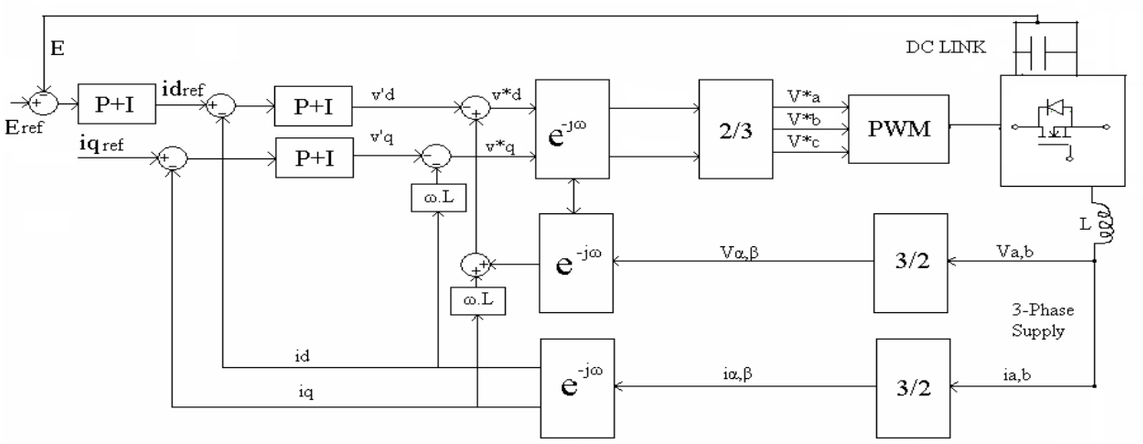

Fig. 11. DQ Control lock diagram.

Each gain in the controller affects the system characteristics differently. Settling time, steady state error and system stability are affected by the amount of the proportional gain. Selecting a large gain attains faster system response, but cost of large overshoot and longer settling time. Application of the integral feedback drives the steady state error to zero. The integral term increases as the sum of the steady state error increases causing the error to eventually be zero. However it can cause overshoot and ringing.

Selection of the two gain constants is critical in providing fast system response with good system characteristics.

The general formulas for DQ transformations are given as follows. We assume that the three-phase source voltages v_a, v_b and v_c are balanced and sinusoidal with an angular frequencyω.

The components of the input voltage phasor along the axes of a stationary orthogonal reference frame (α, β) are given by:

$$v_\alpha = v_a \tag{25}$$

$$v_\beta = \frac{1}{\sqrt{3}} (2 v_b + v_a) \tag{26}$$

The input voltage can then be transformed to a rotating reference frame DQ chosen with the D axis aligned with the voltage phasor. The voltage components are given by:

$$v_d = v_\alpha \cos \omega t - v_\beta . \sin \omega t \tag{27}$$

$$v_q = v_\alpha \sin \omega t + v_\beta \cos \omega t \tag{28}$$

The same transformations are applied to the phase currents.

$$i_d = i_\alpha \cos \omega t - i_\beta . \sin \omega t \tag{29}$$

$$i_q = i_\alpha \sin \omega t + i_\beta \cos \omega t \tag{30}$$

Let v_{a1}, v_{b1} and v_{c1} be the fundamental voltages per phase at the input of the converter.

$$v_a = Ri_a + L\, di_a/dt + v_{a1} \tag{31}$$

$$v_b = Ri_b + L\, di_b/dt + v_{b1} \tag{32}$$

$$v_c = Ri_c + L\, di_c/dt + v_{c1} \tag{33}$$

where L is the value of input line inductance and R is its resistance of the inductor.

Taking the steady state DQ transformation for the inductor, the input voltage to the converter in the DQ reference frame is given by:

$$v_d = Ri_d + L.di_d/dt - \omega Li_q + v_{d1} \tag{34}$$

$$v_q = Ri_q + L.di_q/dt + \omega Li_d + v_{q1} \tag{35}$$

The active and reactive powers are given by:

$$P = v_d.i_d + v_q.i_q \tag{36}$$

$$Q = v_d.i_q - v_q.i_d \tag{37}$$

Inverse DQ transformations then need to be applied to provide the three phase modulating waves (v_{aref}, v_{bref} and v_{cref}) for the PWM generation.

The main advantages of the DQ control are :

1. Direct control the active and reactive power.
2. Fast dynamics of current control loops.

The PWM generator based on a regular asymmetric PWM strategy.

Voltage Control

The DC side may be modelled by a capacitor C, representing the smoothing capacitors, and a resistor R, representing the load. This is shown in Figure 12.

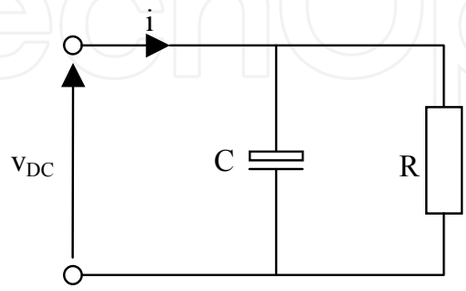

Fig. 12. Schematic of dc voltage link.

The linearised model for the DC side is given by the open-loop transfer function relating the DC link voltage to the supply current:

$$G(s) = \frac{v_{DC}(s)}{i(s)} = \frac{R}{1 + RCs} \tag{38}$$

Applying the PI controller illustrated, i(s) is given by:

$$i(s) = \left(K_p + \frac{K_i}{s} \right)(v_{REF} - v_{DC}) \tag{39}$$

Thus, the closed-loop transfer function is given by:

$$\frac{v_{DC}(s)}{v_{REF}(s)} = \frac{(K_p s + K_i)/C}{s^2 + \frac{s(1 + RK_p)}{RC} + \frac{K_i}{C}} \tag{40}$$

To give a damped response, the poles of the system should be placed along the real axis in the s-domain, i.e. at $s = -\omega_1$ and $s = -\omega_2$, giving the transfer function:

$$\frac{v_{DC}(s)}{v_{REF}(s)} = \frac{(K_p s + K_i)/C}{s^2 + s(\omega_1 + \omega_2) + \omega_1 \omega_2} \tag{41}$$

By equating the coefficients of the denominators of the above equations, the proportional and integral gains are:

$$K_p = C(\omega_1 + \omega_2) - 1/R \tag{42}$$

$$K_i = C\omega_1\omega_2 \tag{43}$$

The zero of the transfer function is where:

$$\left(K_p s + K_i\right)/C = \left(\left(C\left(\omega_1 + \omega_2\right) - 1/R\right)s + C\omega_1\omega_2\right)/C = 0 \tag{44}$$

Therefore:

$$s = \frac{-C\omega_1\omega_2}{C\left(\omega_1 + \omega_2\right) - 1/R} \tag{45}$$

An approach to the controller design is to locate this zero to coincide with one of the poles, say at $s = -\omega_1$, so as to cancel its effect. This gives:

$$\omega_1 = 1/RC \tag{46}$$

The second pole can then be placed at any desired location, to give the desired bandwidth. This gives the proportional and integral gains:

$$K_p = C\omega_2 \tag{47}$$

$$K_i = \omega_2/R \tag{48}$$

Current Control for boost converter

In this case the system is the line from the generator to the input converter, which may be modelled by an inductor in series with a resistor. The generator e.m.f. is assumed to have no dynamic effect, and so is represented as a short circuit. The system schematic is shown in Fig. 13.

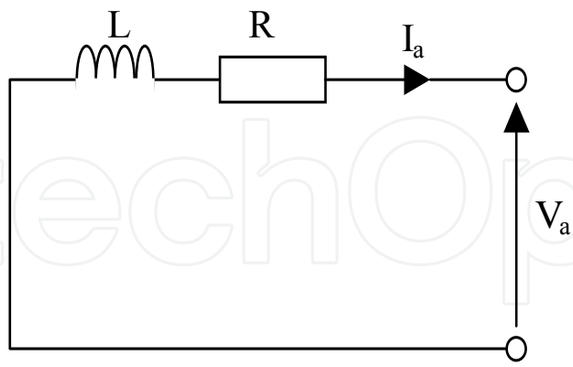

Fig. 13. Schematic of current control for the boost converter.

The phase current is given by:

$$i_a = -\frac{v_a}{R} - \frac{L}{R}\frac{di_a}{dt} \tag{49}$$

The open loop transfer function relating the phase current to the phase voltage is, therefore:

$$\frac{i_a}{v_a} = -\frac{1}{R + Ls} \tag{50}$$

From this simple transfer function, it would appear that the PI controller proposed would suffice, driving the steady-state current error to zero and allowing the behaviour and bandwidth, (i.e. the positions of the poles, of the closed loop system) to be fully determined by choosing the proportional and integral gains. The D-axis and Q-axis currents are compared to their respective demanded values and the error is applied to individual PI controllers to give voltage demands referred to the D-axis and Q-axis. With the feed-forward and dc-coupling terms, the transfer functions of the systems being controlled are:

$$\frac{i_d(s)}{v_d'(s)} = \frac{1}{Ls + R} \tag{51}$$

$$\frac{i_q(s)}{v_q'(s)} = \frac{1}{Ls + R} \tag{52}$$

Again, these are first-order equations and similar to the voltage control loop, the PI controllers will drive the steady-state error to zero and enable the behaviour and bandwidth of the closed-loop system to be determined by placing the poles appropriately.

Current Control for buck converter

The idea of controlling the current of the AC side LC filter has been proposed as a way of suppressing the excitation of the resonance of this filter. In steady state and in the absence of distortion there are no current components to excite the resonance because the resonant frequency will have been chosen to fall between the fundamental and the switching frequency. During the transient, the resonance of the filter can be damped by choosing the characteristics impedance to match the resistance and the inductance.

In this case the system is the line from the generator to the input converter, which may be modeled by an inductor in series with a resistor and capacitor.. The system schematic is shown in Figure 14.

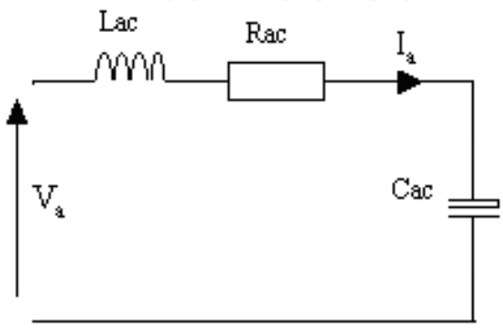

Fig. 14. Schematic of current control for the buck converter.

The open loop transfer function relating the phase current to the phase voltage is, therefore:

$$G(s) = \frac{1}{s^2 L_{ac}C_{ac} + sR_{ac}C_{ac} + 1} \tag{53}$$

From this transfer function it would be appear that the PI controller proposed would suffice, driving the steady state error to zero and allowing the behaviour and bandwidth (position of the poles) of closed loop system to be fully determined by choosing the proportional and integral gains. The procedure for this is the same as that described above for voltage control.

6. Hardware design

All of the converters components had to be selected so that normal service maintenance would ensure the retention of their specified characteristics through the full range of operational and environmental conditions likely to be encountered through the life of the aircraft, or support facility, in which they are installed (Taha M 1999).

6.1 Capacitors

The choice of capacitors is very important for aerospace industry. Wet aluminum electrolytic capacitors are not suitable due to their limited operating temperature range and hence limited life. Equivalent series resistance is also a problem for these and other types of electrolytic capacitor and therefore alternative technologies, such as ceramic or plastic, are recommended.

Ceramic capacitors have a good lifetime, low series resistance and they work in high temperature conditions. On the other hand for a rating of a few hundred volts this type of capacitor has a very small value per unit volume and are only available in units of up to 20uF. The size and weight for this converter are very important. Therefore care was taken to choose the optimal value of the DC capacitor

6.2 Magnetic components

Another important factor is the design of the magnetic components. In order to achieve a small air gap, minimum winding turns, minimum eddy current losses and small inductor size, the inductor should be designed to operate at the maximum possible flux density. Also, care should be taken to ensure that the filter inductors do not reach a saturated state during the overload condition. As the cores saturate, the inductance falls and the THD rises.

7. Simulation results for boost and buck converter

The power conversion in the boost or buck converter is exclusively performed in switched mode. Operation in the switch mode ensures that the efficiency of the power conversion is high. The switching losses of the devices increase with the switching frequency and this should preferably be high in order have small THD therefore choosing the switching frequency poses significant challenges due to:

1. Supply frequency Variation (360 to 800 Hz).

For the boost converter the simulation carried out with a fixed switching frequency. However, for the buck converter. one of the method could be used is a variable switching frequency

which depend on the input frequency. Trade off between the values of the filters and the switching frequency have been studies, in order to maintain the THD within the required value at different input frequency. Another method is to use the same switching frequency for different input frequency, here the highest input frequency should be considered.

The parameter values used for the simulation are shown in table 1. Fig. 15 to fig. 18 show, input AC voltage and current and Dc output voltage.

Boost converter	Buck converter
RMS phase voltage = 115 V	RMS phase voltage = 115 V
DC voltage setting = 400 V	DC voltage setting = 42 V
AC Input Filter = L_{ac}= 100uH	AC Input Filter = L_{ac}= 150uH; C_{ac} = 1µF
Dc Output filter C_{dc} = 50µF	Dc Output filter = L_{dc} = 1mH ; C_{dc} = 50µF
Load = 10 Ω	Load = 0.5 Ω
Switching freq for 800 input freq =20000 Hz	Switching freq for 800 input freq =33600 Hz
Switching freq for 360 input freq =20000 Hz	Switching freq for 360 input freq =23760 Hz

Table 1. Simulation parameters.

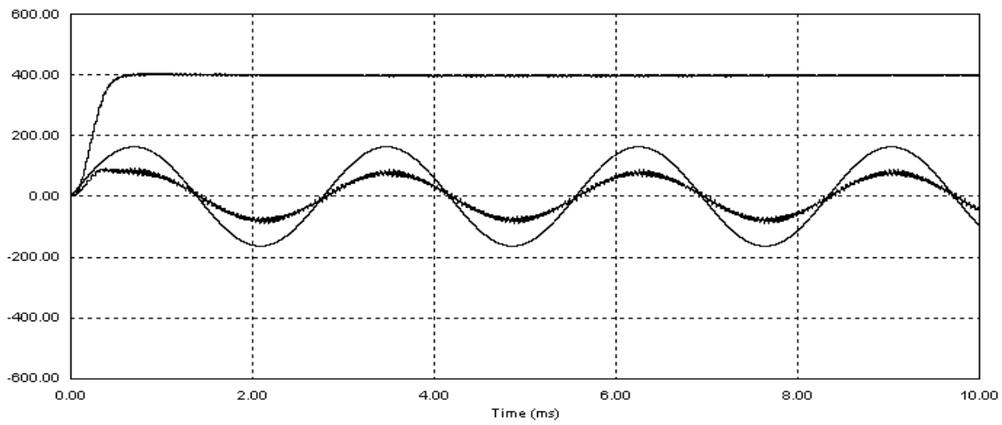

Fig. 15. Boost converter simulation results at 360 Hz input frequency.

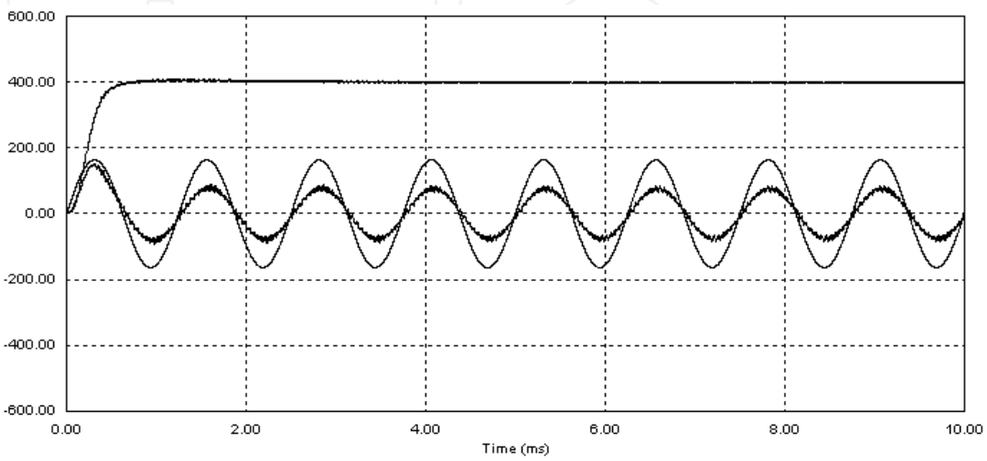

Fig. 16. Boost converter simulation results at 800 Hz input frequency.

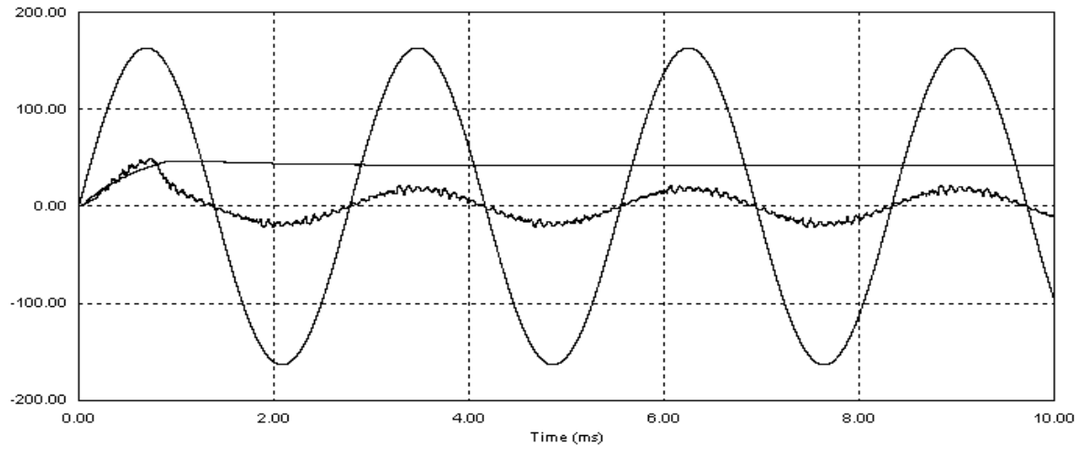

Fig. 17. Buck converter simulation results at 360 Hz input frequency.

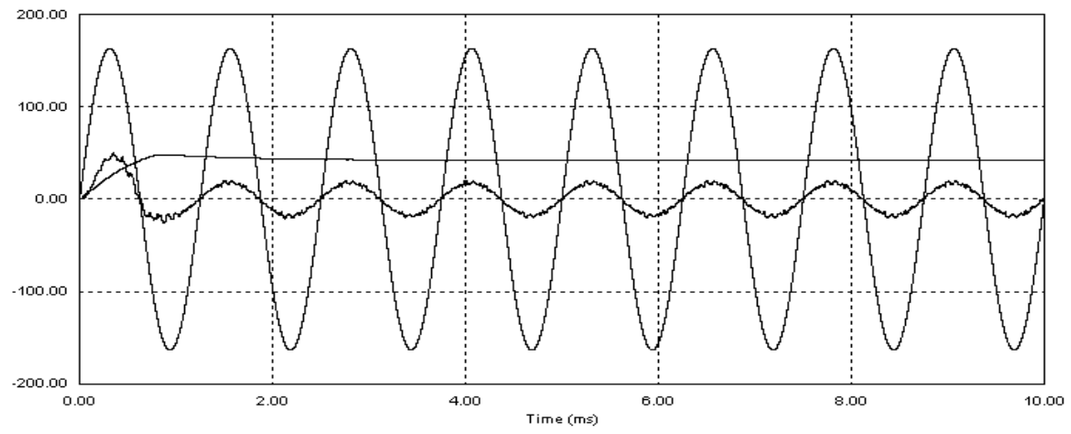

Fig. 18. Buck converter simulation results at 800 Hz input frequency.

8. Simulation results for the adaptive power control

Simulation has been done at 16 kW approximately. Fig. 19 shows the "per phase" parameter values used. Fig. 20 and fig. 21 show results for 360 Hz, the voltage drops to 107.5 V at the input filter of the converter. To compensate for the voltage drop across the cable, q (reactive demand) has been set this gave leading power factor. Fig. 21 shows that the voltage Va3 increase to 111.3 V at 0.9 PF.

Fig. 22 and Fig. 23 show results for 800 Hz, the voltage drops to 106 V at the input filter of the converter. Fig. 23 shows that the voltage Va3 increase to 1113 V at 0.9 PF.

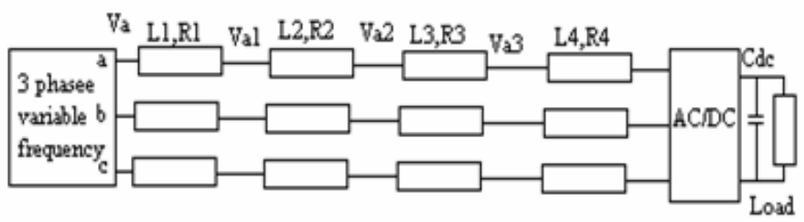

V_{a1} is the point of regulation voltage
V_{a3} is the point of connection of the load
L_1 = 25uH,R_1= 0.015 ohms is the generator inductance and resistance.
L_2 = 10uH,R_2= 0.01 ohms is the cable inductance and resistance from the generator to contactor.
L_3 = 20uH,R_2= 0.1 ohms is the cable inductance and resistance from the contactor to the load.
L_4 = 100uH,R_4= 0.1 ohms is the inductance and resistance of the load converter input filter.

Fig. 19. Single phase parameters for the adaptive power control.

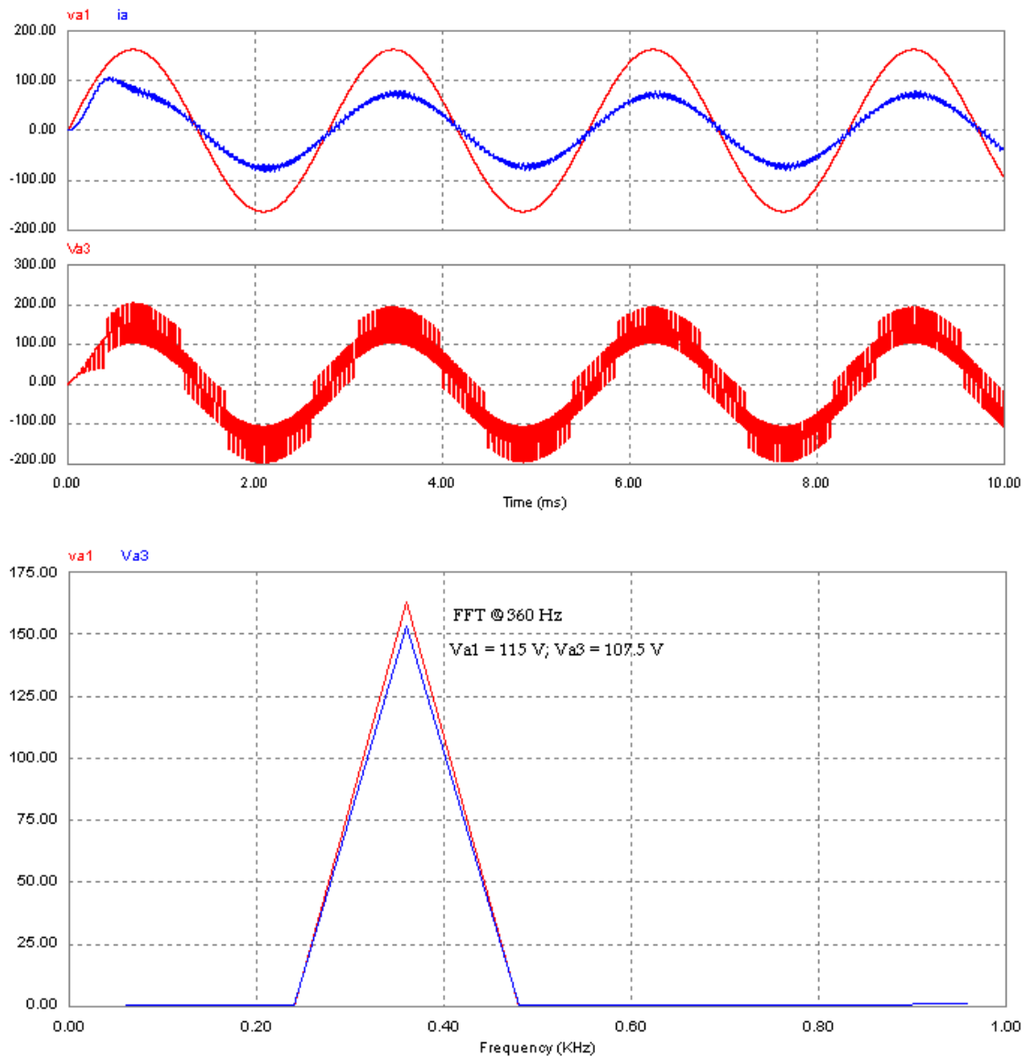

Fig. 20. Results at 360 Hz input frequency for unity power factor.

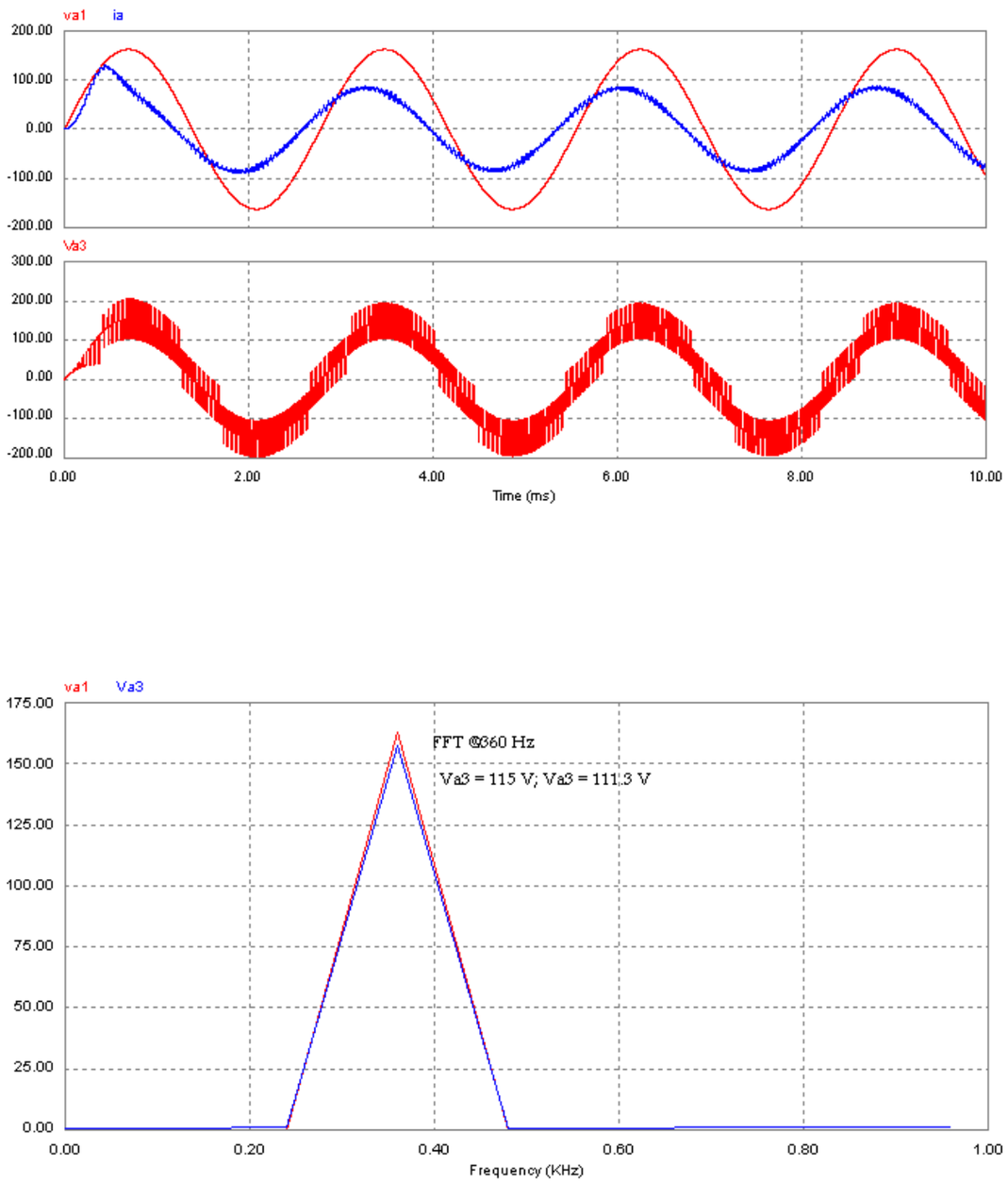

Fig. 21. Results at 360 Hz input frequency for 0.9 power factor.

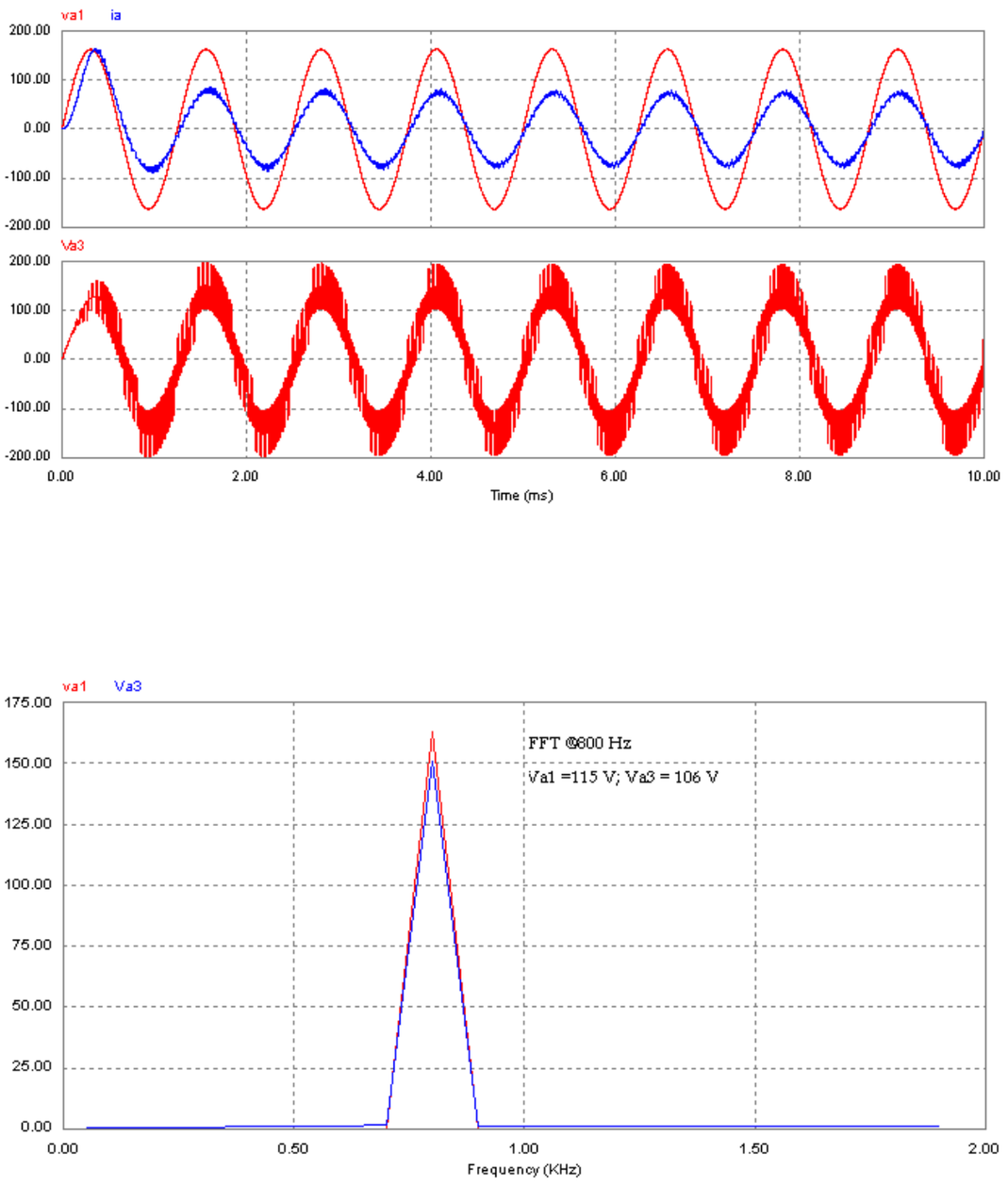

Fig. 22. Results at 800 Hz input frequency for unity power factor.

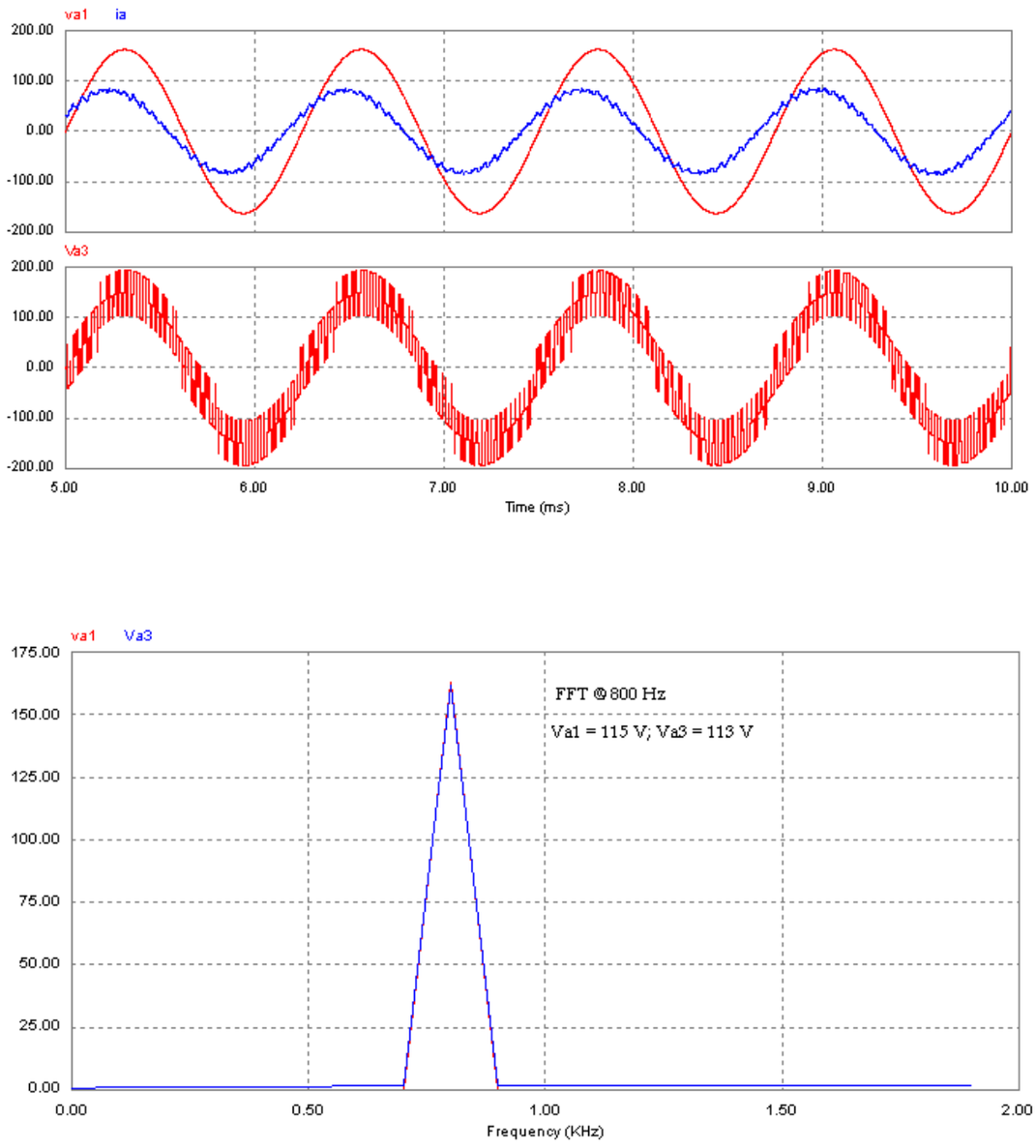

Fig. 23. Results at 800 Hz input frequency for 0.9 power factor.

9. Conclusion

On the basis of the space vector concept a PWM controller was developed. It has been shown that sinusoidal modulation generated in a space vector representation with PI controllers give an adequate performance in steady state and transient condition fast. It has been shown that with the future use of advanced power electronic converters within aircraft equipment, there is the possibility to operate these at variable input frequency and keeping the input current harmonics low.

An AC/DC buck and boost converters with different input frequency and offers low THD (less than 7%) has been described and simulated.

The operation and performance of the proposed topology was verified by simulating a 16 KW with a pure resistive load of 10 Ω and 400 dc voltage for the boost converter and a 3.5 KW with a pure resistive load of 0.5 Ω and 42 dc voltage for the buck converter. The input current is sinusoidal and power factor is unity. The DC voltage is well smoothed.

With the future use of advanced power electronic converters such as active rectifiers and matrix converters within aircraft equipment, there is the possibility to operate these at variable power factor in order to provide system level benefits. These include control of the voltage at the load and improvements in power factor seen at the POR.

10. Acknowledgment

I would like to express my sincere appreciation and respect to the late Prime Minister Rafik El hariri who is entirely responsible for funding my studies in England.

11. References

Faleiro, L. (2005). Beyond the More Electric Aircraft, *Aerospace America,* September 2005, pp 3540

Green, A.; Boys J. & Gates G. (1988). 3-phase voltage sources reversible rectifier, *IEE Proceeding* ,1988,135, pp 362-370, 2002

Green T.; Taha M.; Rahim N.; &Williams B.W. (1997). Three Phase Step-Down Reversible AC-DC Power converter, *IEEE Trans. Power Electron*, 1997,12, pp 319-324

Habetler T. (1993). A space Vector-Bases Rectifier Regulator for AC/DC/AC Converters. I*EEE Trans. Power Electron*, 1993 Vol 8, pp. 30-36

Kazmierkowski M.; Dzeiniakowski M.& Sulkowski W. (1991). Novel space vector based current control for PWM inverters, *IEEE Trans. Power Electron*, 1991, 6, pp 158-166

Taha M (1999). "Power electronics for aircraft application" *Power electronics for demanding applications colloquium, IEE,April 1999, 069 pp 5 -8*

Taha M.; Skinner D.; Gami S.; Holme M. & Raimondi G (2002); *Variable Frequency to constant frequency converter (VFCF) for aircraft application*, PEMD 2002.

Taha M. (2008). Mitigation of Supply Current Distortion in 3- Phase /DC Boost converters For Aircraft Applications*, PEMD 2008.*

Taha, M (2007). Active rectifier using DQ vector control for aircraft power system, *IEMDC 2007* pp 1306-1310

Taha M, Trainer R D (2004); Adaptive reactive power control for aircraft application Power Electronics, Machines and Drives, 2004. (PEMD 2004). Second International Conference on (Conf. Publ. No. 498) 2:469- 474 Vol.2.

Weimer J. (1995). Powe Managemennt and Distribution for More Electric Aircraft, *Proceeding of the 30th Intersociety Energy Conversion Engineering Conference*,pp.273-277

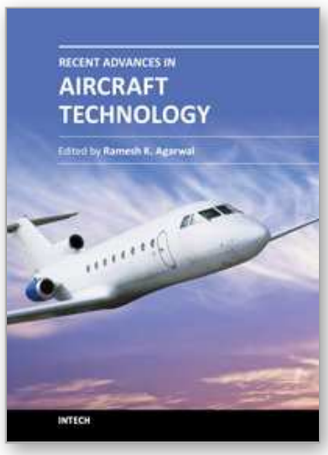

Recent Advances in Aircraft Technology

Edited by Dr. Ramesh Agarwal

ISBN 978-953-51-0150-5
Hard cover, 544 pages
Publisher InTech
Published online 24, February, 2012
Published in print edition February, 2012

The book describes the state of the art and latest advancements in technologies for various areas of aircraft systems. In particular it covers wide variety of topics in aircraft structures and advanced materials, control systems, electrical systems, inspection and maintenance, avionics and radar and some miscellaneous topics such as green aviation. The authors are leading experts in their fields. Both the researchers and the students should find the material useful in their work.

InTech Europe
University Campus STeP Ri
Slavka Krautzeka 83/A
51000 Rijeka, Croatia
Phone: +385 (51) 770 447
Fax: +385 (51) 686 166
www.intechopen.com

InTech China
Unit 405, Office Block, Hotel Equatorial Shanghai
No.65, Yan An Road (West), Shanghai, 200040, China
中国上海市延安西路65号上海国际贵都大饭店办公楼405单元
Phone: +86-21-62489820
Fax: +86-21-62489821

IntechOpen